



ELSEVIER

Available online at [www.sciencedirect.com](http://www.sciencedirect.com)

SCIENCE @ DIRECT®

Carbohydrate Research 338 (2003) 415–421

CARBOHYDRATE  
RESEARCH[www.elsevier.com/locate/carres](http://www.elsevier.com/locate/carres)

# Characterizing the pH-dependent stability and catalytic mechanism of the family 11 xylanase from the alkalophilic *Bacillus agaradhaerens*

David K.Y. Poon,<sup>a</sup> Philip Webster,<sup>b</sup> Stephen G. Withers,<sup>a,b,d,\*</sup>  
Lawrence P. McIntosh<sup>a,b,c,d,\*</sup>

<sup>a</sup>The Department of Chemistry, University of British Columbia, Vancouver, BC, Canada V6T 1Z1

<sup>b</sup>The Department of Biochemistry and Molecular Biology, University of British Columbia, Vancouver, BC, Canada V6T 1Z1

<sup>c</sup>The Biotechnology Laboratory, University of British Columbia, Vancouver, BC, Canada V6T 1Z1

<sup>d</sup>The Protein Engineering Network of Centres of Excellence, University of British Columbia, Vancouver, BC, Canada V6T 1Z1

Received 24 October 2002; accepted 15 November 2002

## Abstract

The xylanase, BadX, from the alkalophilic *Bacillus agaradhaerens* was cloned, expressed and studied in comparison to a related family 11 xylanase, BcX, from *B. circulans*. Despite the alkaline versus neutral conditions under which these bacteria grow, BadX and BcX both exhibit optimal activity near pH 5.6 using the substrate *o*-nitrophenyl  $\beta$ -xylobioside. Analysis of the bell-shaped activity profile of BadX yielded apparent  $pK_a$  values of 4.2 and 7.1, assignable to its nucleophile Glu94 and general acid Glu184, respectively. In addition to having an  $\sim 10$ -fold higher  $k_{cat}/K_m$  value with this substrate at pH 6 and 40 °C, BadX has significantly higher thermal stability than BcX under neutral and alkaline conditions. This enhanced stability, rather than a shift in its pH-optimum, may allow BadX to hydrolyze xylan under conditions of elevated temperature and pH. © 2003 Elsevier Science Ltd. All rights reserved.

**Keywords:** Bacillus xylanase; Glycosidase; pH-Dependent mechanism; Protein stability; Extremophile

## 1. Introduction

The use of xylanases is becoming increasingly important in the pulp and paper industry. During the bleaching process, removal of lignin can be facilitated by hydrolysis of xylan, the major component of hemicellulose. Xylanases specifically degrade xylan, thereby allowing the use of significantly smaller amounts of environmentally toxic chlorinated chemicals. Since elevated temperatures and pH are used in the pulping and bleaching process, the ideal xylanase for this purpose should be highly thermostable and active under alkaline solutions.<sup>1,2</sup>

As summarized in several reviews,<sup>2–4</sup> low-molecular weight xylanases from the family 11 of glycoside hydrolases (EC 3.2.1.8; CAZY database: <http://afmb.cnrs-mrs.fr/CAZY/index.html>)<sup>5,6</sup> have been isolated from a plethora of bacteria and fungi, many of which grow under extreme conditions. Remarkably, these enzymes have been reported to exhibit pH optima ranging from 2 to at least 9. Given the highly conserved sequences of these homologous xylanases, as well as their common double-displacement catalytic mechanism,<sup>7</sup> this prompts the question as to what factors establish such an apparently dramatic range of pH-dependent enzymatic activities.

Previously, we characterized the family 11 xylanase from *B. circulans* (BcX) and investigated its pH-dependent activity by a combination of kinetic, structural and <sup>13</sup>C NMR studies.<sup>8,9</sup> The acidic limb of the bell-shaped pH-activity profile of BcX was assigned to the deprotonation of Glu78 ( $pK_a$  4.6), as required to form a

\* Corresponding authors. Tel.: +1-604-822-3402; fax: +1-604-822-8869 (S.G.W.); Tel.: +1-604-822-3341; fax: +1-604-822-5227 (L.P.M)

E-mail addresses: [withers@chem.ubc.ca](mailto:withers@chem.ubc.ca) (S.G. Withers), [mcintosh@otter.biochem.ubc.ca](mailto:mcintosh@otter.biochem.ubc.ca) (L.P. McIntosh).

catalytic nucleophile, while the basic limb was assigned to Glu172 ( $pK_a$  6.7). This latter group must remain protonated to act as the general acid during the rate-limiting glycosylation step of the hydrolytic reaction followed by this retaining glycosidase. Furthermore, substitution of Asn35 with Asp reduced the pH optimum of BcX from 5.7 to 4.6, combined with an  $\sim 20\%$  increase in activity.<sup>10</sup> A detailed study of this mutant enzyme demonstrated that a reverse protonation mechanism, coupled with the formation of a strong hydrogen bond between Asp35 and Glu172 in the glycosyl-enzyme intermediate, leads to the shift in its pH optimum. In combination with research by several groups,<sup>11–13</sup> this work provided an explanation for the well-established observation that family 11 xylanases with pH optima  $< 5$  have an aspartic acid adjacent to their general acid/base catalytic residue, while those with optima  $> 5$  have an asparagine. However, no further patterns of sequence conservation have been identified for xylanases with significantly alkaline pH optima.

To investigate this question, we turned to the 23 kDa xylanase, BadX, from the alkalophilic *Bacillus agaradhaerens*. This bacterium, which can be isolated from highly alkaline sources such as soda lakes, produces many glycoside hydrolases that are of interest due to their apparent catalytic activities under conditions of elevated pH.<sup>14</sup> For example, a pH-optimum of 7–8 towards xylan has been reported for BadX.<sup>15</sup> The high-resolution tertiary structures of BadX (also referred to as Xyl11) in its glycosyl-enzyme intermediate and product-bound states have been determined, confirming that the enzyme follows a retaining mechanism<sup>16,17</sup> with a striking similarity to that observed for BcX.<sup>18,19</sup> Here, we present a characterization of BadX in terms of its kinetic behaviour and thermal stability. Consistent with their highly conserved structures, the pH-dependent activity profile of BadX resembles that of BcX, with both xylanases having pH optima near 5.6. However, BadX exhibits dramatically enhanced thermal stability, which may account for its catalytic activity under conditions of elevated pH and temperature.

## 2. Results

### 2.1. $k_{cat}$ and $K_m$ values of BadX

The Michaelis–Menten kinetic parameters,  $k_{cat}$  and  $K_m$ , were determined for BadX at pH 6.0 and 40 °C to be  $16.9 \text{ s}^{-1}$  and 2.6 mM, respectively, using the synthetic substrate *o*-nitrophenyl  $\beta$ -xylobioside, ONPX<sub>2</sub> (Fig. 1). By comparison, values of  $7.1 \text{ s}^{-1}$  and 14.6 mM (which agree with those previously reported<sup>20</sup>) were determined for BcX under identical conditions. Thus BadX exhibits an  $\sim 10$ -fold greater second-order rate constant,  $k_{cat}/K_m$ , than BcX towards this defined substrate.

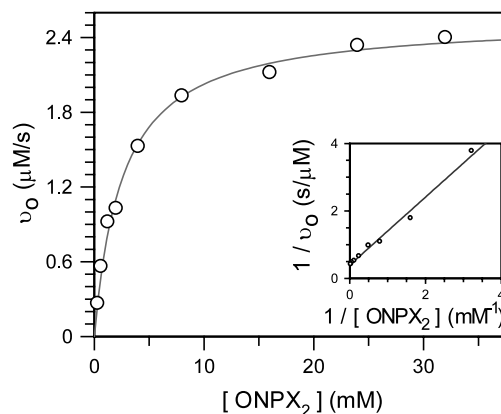


Fig. 1. Michaelis–Menten and Lineweaver–Burke (inset) plots for the hydrolysis of *o*-nitrophenyl  $\beta$ -xylobioside (ONPX<sub>2</sub>) by  $1.5 \times 10^{-4}$  mM BadX at 40 °C and pH 6.0. Fitting of the initial reaction velocity  $v_0$  versus substrate concentration yielded  $k_{cat} = 16.9 \text{ s}^{-1}$  and  $K_m = 2.6 \text{ mM}$ .

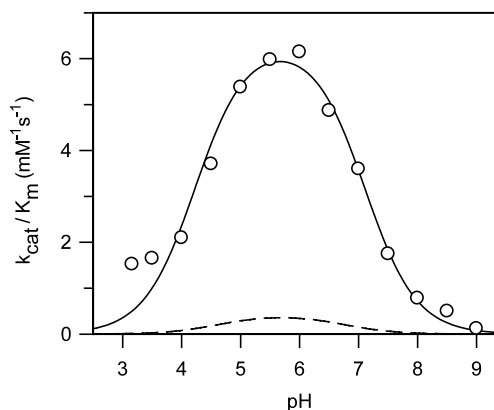


Fig. 2. Dependence of  $k_{cat}/K_m$  upon pH for the hydrolysis of ONPX<sub>2</sub> at 25 °C by BadX. Fitting (solid line) of the data points (o) yielded apparent  $pK_a$  values of 4.2 and 7.1. The pH-dependent profile of BcX (dashed line) was calculated using data from Ref. 8.

### 2.2. pH-Dependent activity

The pH-dependence of  $k_{cat}/K_m$  for the hydrolysis of ONPX<sub>2</sub> by BadX follows a bell-shaped curve with an optimum value at pH 5.6 (Fig. 2). Fitting of this curve to the equation for two ionization equilibria yielded apparent  $pK_a$  values of 4.2 and 7.1 for the acidic and basic limbs, respectively. This behavior is similar to that found previously for BcX,<sup>8</sup> with a pH optimum of 5.7 and apparent  $pK_a$  values of 4.6 and 6.7.

### 2.3. Thermal stability

The stability of BadX and BcX towards thermal denaturation was monitored by CD spectroscopy. As previously noted for BcX, neither protein completely refolds reversibly after thermal or denaturant-induced unfolding under a wide variety of buffering conditions.<sup>20–22</sup>

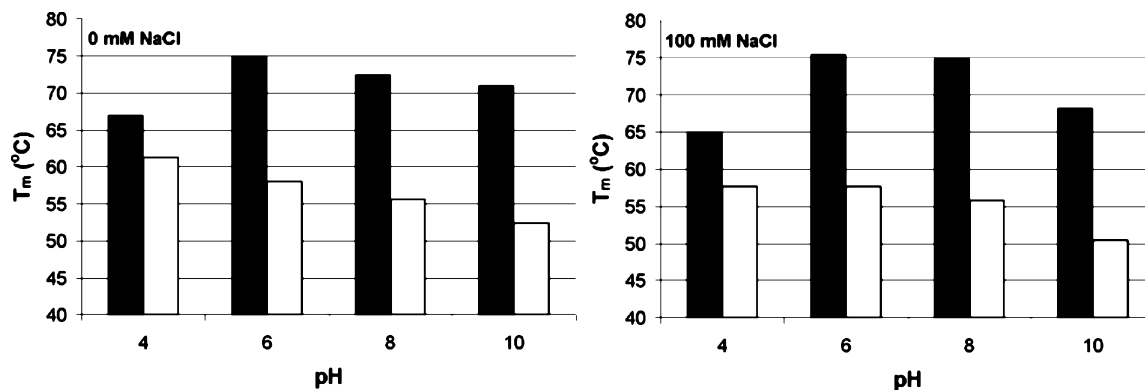


Fig. 3. The midpoint denaturation temperatures ( $T_m$ ) of BadX (■) and BcX (□) in 10 mM sodium phosphate and 0 or 100 mM NaCl as a function of sample pH.

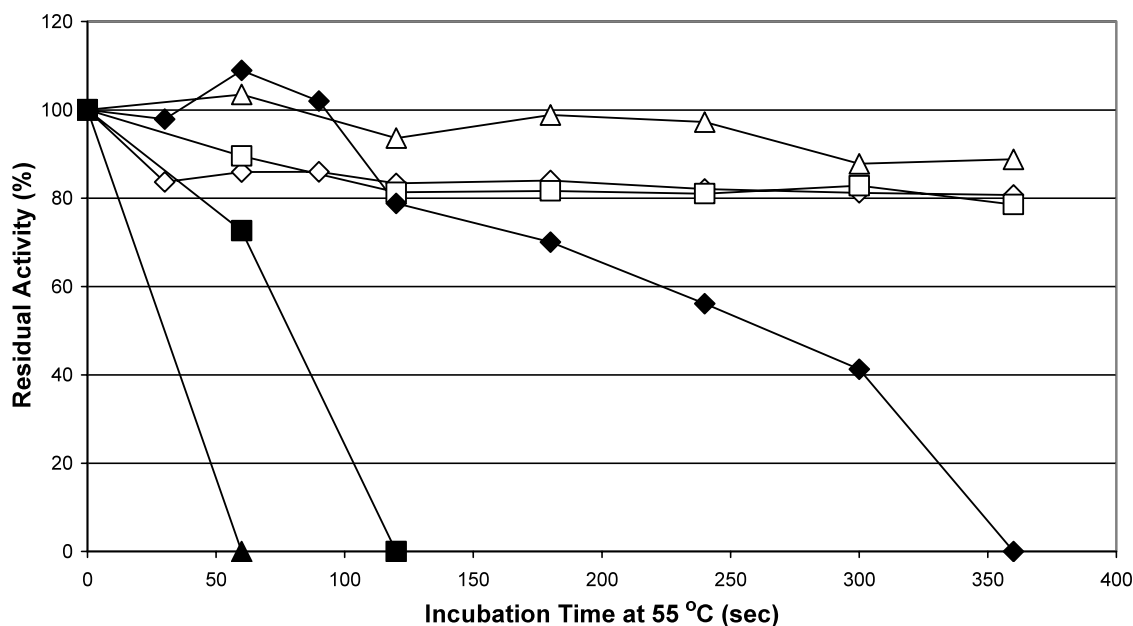


Fig. 4. The normalized residual activity of BadX (◇, □, △) and BcX (◆, ■, ▲) as a function of incubation time at 55 °C and pH 6 (◇, ◆), 8 (□, ■) and 10 (△, ▲). Sample aliquots were quenched on ice and assayed at 20 °C and pH 6 using ONPX<sub>2</sub>. Lines on the plot are drawn to guide the eye.

Therefore, data reported in Fig. 3 reflect apparent midpoint unfolding temperatures and, while a reliable monitor of relative stability, do not allow calculations of reversible thermodynamic parameters. At pH 2.0, both BadX and BcX are partially unfolded or aggregated, as evident by their broad thermal transitions (not shown). At pH 4 and above, BadX consistently denatures ~6 to 20 °C higher than BcX, and the addition of 100 mM NaCl does not markedly change this pattern. Similar unfolding temperatures were measured for BcX by calorimetry.<sup>21</sup>

#### 2.4. Irreversible denaturation

As a complementary approach towards thermal unfolding studies, the resistance of each xylanase towards

irreversible loss of activity was measured by incubation at 55 °C and pH 6.0, 8.0 or 10.0, followed by quenching on ice and assaying at pH 6.0 and 20 °C. As summarized in Fig. 4, BadX retains >80% of its activity after incubation for 6 min under these conditions, whereas BcX is irreversibly inactivated at a rapid rate that increases with pH.

### 3. Discussion

#### 3.1. Enzymatic activity

Through a combination of increased  $k_{cat}$  and decreased  $K_m$  values, BadX exhibits ~10-fold higher activity ( $k_{cat}/K_m$ ) towards a defined xylobioside substrate than

does BcX. This small, albeit significant, effect must arise through subtle differences between these two xylanases, as the residues composing their active site clefts are highly conserved in both sequence and structural arrangement (e.g., comparing Protein Data Bank coordinate files 1QH7/1XNB, 1HYG/1BVV and 1HYH/1XNA for the free, covalent glycosyl-enzyme intermediate and mutant product complexes of BadX/BcX, respectively). One interesting exception to this sequence conservation is the functional substitution of Tyr166 in BcX by a Glu178-Arg49 ion pair in BadX. In the case of BcX, Gln7 and Tyr166 hydrogen bond to O2 and O3 of the xylosyl group in the  $-2$  subsite of the substrate binding cleft, whereas with BadX, Glu17 and Arg49 complete these interactions.<sup>17,18</sup> This latter network of charged hydrogen bonds could result in the  $\sim$  fivefold lower  $K_m$  value measured for BadX than BcX towards ONPX<sub>2</sub>.

The pH-dependent activity profiles of BadX and BcX are comparable (Fig. 2), with both enzymes having pH-optima near 5.6. Based on the homologous structures and common catalytic mechanisms of the two family 11 xylanases, we assign the gain in activity of BadX with increasing pH to the deprotonation of the nucleophile Glu94 ( $pK_a$  4.2) and the subsequent loss of activity to that of the general acid Glu184 ( $pK_a$  7.1). The similarity of these apparent  $pK_a$  values with those of 4.6 and 6.7 measured previously for BcX<sup>8</sup> is consistent with the strict conservation of the residues immediately surrounding the two catalytic glutamic acids. These amino acids, which include Asn35, Tyr69, Tyr80, Arg112 and Gln127, have been shown by mutagenesis to help establish the precise  $pK_a$  values of Glu78 and Glu172 in BcX.<sup>9</sup> Electrostatic calculations<sup>9</sup> also predict that the Glu94 and Glu184 in BadX have comparable values to those of their counterparts in BcX (not shown).

Previously, a pH optimum between 7 and 8 was reported for a crude preparation of BadX towards a dyed xylan substrate.<sup>15</sup> The discrepancy with the results of this current study may arise from several sources, such as their use of a partially purified bacterial extract, which may contain additional glycosidase activities, or the use of a complex substrate, which itself may have pH-dependent properties. Interestingly, the family 11 xylanase XylJ from the alkalophilic *Bacillus* sp. 41M-1 has also been reported to have a very broad pH-dependent activity profile towards xylan with a pH optimum at 9.<sup>23</sup> Based on the hydrolytic mechanism employed by these retaining xylanases, this would require that a catalytic glutamic acid residue in XylJ has a remarkable  $pK_a > 9$  in order to serve as a general acid. Given that BadX and XylJ are highly homologous, with  $\sim$  95% sequence similarity across their catalytic domains<sup>24</sup> and no significant amino acid substitutions near their active site clefts, it remains to be established as to what

features, if any, contribute to this reported high pH activity.

### 3.2. Thermal stability

In contrast to their comparable enzymatic properties, BadX is significantly more stable than BcX, as demonstrated by both thermal unfolding studies and by kinetic measurements of irreversible enzyme inactivation. This enhanced stability may arise from several sources. First, BadX (206 residues) contains two small N-terminal  $\beta$ -strands, as well as an internal  $\alpha$ -helical turn and C-terminal  $\beta$ -hairpin<sup>25</sup> not present in BcX (185 residues). The potential importance of the former feature is highlighted by the enhanced stability of the mesophilic *Streptomyces lividans* xylanase B resulting from exchange via gene shuffling of the N-terminal sequence from the thermophilic *Thermomonospora fusca* xylanase A,<sup>26</sup> and by the stabilization of BcX upon fusion to the N-terminal sequence of this *T. fusca* enzyme.<sup>27</sup> On a more precise level, mutation of Thr11 to Tyr in the mesophilic *Streptomyces* sp. S38 xylanase led to its enhanced stability, possibly by formation of a favourable perpendicular aromatic–aromatic ring interaction with Tyr16.<sup>28</sup> Such an interaction is seen in the crystal structure of the thermophilic *Thermomyces lanuginosus* xylanase<sup>29</sup> and in a model of *T. fusca* xylanase A.<sup>28</sup> Interestingly, this potentially-stabilizing aromatic–aromatic interaction, which bridges a conserved Type I' turn found in family 11 xylanases containing the extra N-terminal  $\beta$ -strand(s), may be replaced functionally in BadX by a weakly hydrogen-bonded Asn-Asp pair. Second, in addition to having several distinct features including an amide–aromatic hydrogen bond,<sup>30</sup> a buried His residue adjacent to a bound internal water molecule,<sup>31</sup> and a buried Asp-Arg ion pair<sup>32</sup> characterized previously in BcX, BadX has three additional ionizable residues in solvent-inaccessible environments: Lys50, His60 and Glu178. Of these, the first is hydrogen-bonded to a presumably neutral His11, whereas the latter two form ion pairs with Glu167 and Arg49, respectively. Such electrostatic interactions within the low dielectric interior of a protein can contribute significantly to the specificity and stability of its folded state.

In addition to such defined and experimentally testable interactions, the enhanced stability of BadX relative to BcX may also arise from changes in overall amino acid composition. In a recent structural genomics-based comparison of homologous proteins from thermophilic and mesophilic organisms, several global trends were correlated with elevated stability, such as an increased number of salt bridges and a greater number of charged amino acid residues, yet smaller number of polar non-charged residues, in exposed surface regions.<sup>33</sup> These trends are followed in the case of

BadX, with 17.4% of its total amino acids being ionizable (vs. 12.4% in BcX), and of its exposed side chains, 25% are charged (vs. 16% in BcX) and 49% are polar (vs. 55% in BcX).

### 3.3. Summary

The mode of action of many xylanases requires that they be secreted extracellularly. The fact that *B. agaradhaerens* grows in alkaline environment<sup>14</sup> prompts the question as to how BadX may function under conditions of high pH, either found naturally or used in industrial processes such as the pre-treatment of pulp.<sup>15</sup> Our studies reveal that, despite its source, this enzyme has a pH optimum at 5.6 and thus does not exploit any specific electrostatic mechanisms to significantly elevate the  $pK_a$  values of its catalytic residues beyond that found for related family 11 xylanases such as BcX. Based on its measured pH-activity profile, BadX retains ~10% and 0.1% of its maximal activity at pH 8 and 10, respectively. Combined with an Arrhenius-type increase in reaction rates with temperature, this level of activity may still allow the thermally stable BadX to adequately catalyze the hydrolysis of xylan under extreme natural or industrial conditions.

## 4. Experimental

### 4.1. General

ONPX<sub>2</sub> was synthesized according to published procedures.<sup>34,35</sup> All other chemicals were obtained from Sigma Chemical Co. unless otherwise stated.

### 4.2. Molecular biology, enzyme expression and purification

The gene for BadX (Genbank accession A68006) was cloned by PCR methods from *B. agaradhaerens* AC13 (ATCC strain # 700163; cultured in 0.5% peptone, 0.3% yeast extract and 0.5% NaCl at pH 9.7 and 30 °C) into the *Nco*I and *Nhe*I restriction sites of the pET28 vector (Stratagene). The resulting construct encoded an N-terminal metal affinity tag and thrombin cleavage site (MGSSHHHHHSSGLVPRGSHMASA) followed by residues Ile2 through Ser207 of the BadX catalytic domain. The sequence and numbering scheme corresponds exactly to that of the BadX construct (also referred to as Xyl11) used to obtain the Protein Data Bank co-ordinate file 1QH7.<sup>16,17</sup> Absent from the predicted sequence of the full-length protein are an N-terminal secretory leader sequence and a disordered 14 residue C-terminal extension.<sup>†</sup>

BadX was prepared starting with a 25 mL overnight culture of the transformed *E. coli*, grown at 37 °C in LB media with 35 mg/L of kanamycin. An aliquot (10 mL) of the overnight culture was used to inoculate 1 L of LB media containing 35 mg/L of kanamycin, and the cells were grown with shaking at 37 °C to an optical density (OD<sub>600</sub>) between 0.5 and 1.0. Protein expression was induced with 0.75 mM isopropyl β-D-thiogalactoside followed by growth at 30 °C for 3 h. The cells were collected by centrifugation (7000 rpm, 10 min) and re-suspended in ~30 mL of nickel column binding buffer (5 mM imidazole, 50 mM HEPES, 500 mM NaCl and 5% glycerol at pH 7.5) and 25 mg (1/4 tablet) of Complete™ protease inhibitor cocktail (Roche). The resultant cellular suspension was then passed through a French-press cell at 10,000 psi and sonicated for 10 min to ensure complete lysis. After centrifugation at 15,000 rpm for 1 h, the BadX was purified by nickel affinity chromatography using the above nickel column buffers with 5 mM imidazole for binding, 60 mM imidazole for washing and 250 mM imidazole for elution. The His-tag on BadX was cleaved by thrombin (Roche) during an overnight dialysis into 10 mM sodium phosphate at 4 °C and pH 6. The thrombin was inactivated by the addition of *p*-aminobenzamide immobilized on cross-linked 4% beaded agarose, and the free His-tag as well as any uncleaved protein was removed via passage over a nickel column. The resultant purified BadX was concentrated using a 3 kDa nominal cut-off stirred ultrafiltration cell (Amicon Corp.) and exchanged into a final buffer of 10 mM sodium phosphate at pH 6. The protein had a molecular weight of 23,673 Da measured by electrospray ionization mass spectrometry. This agrees with the predicted value of 23,665 Da for residues 2–207 of the catalytic domain of BadX, plus an N-terminal extension of GSHMASA remaining after thrombin cleavage of the affinity tag. The enzyme concentration was determined spectrophotometrically using a predicted value of  $\epsilon_{280\text{nm}} = 56,470 \text{ M}^{-1} \text{ cm}^{-1}$  (ExpASy website: <http://ca.expasy.org/tools/protpar-ref.html>).<sup>36</sup>

The expression and purification of BcX were performed according to published protocols.<sup>10,37</sup> The sequence and numbering scheme is that of the Protein Data Bank coordinate file 1XNB.<sup>18,19</sup>

### 4.3. Steady-state enzyme kinetics

All spectrophotometric experiments were performed using 1 cm pathlength micro quartz cuvettes with a Unicam 8700 UV–Vis spectrophotometer equipped with a circulating water bath. The determination of the Michaelis–Menten steady-state parameters  $k_{\text{cat}}$  and  $K_m$  of both BadX and BcX and the pH-dependence of BadX were performed according to published protocols.<sup>10</sup> The hydrolysis of ONPX<sub>2</sub> and the release of the

<sup>†</sup> G. Davies, personal comm.

nitrophenyl chromophore was monitored at 400 nm while the steady-state kinetic data were fitted using the program GraFit.<sup>38</sup>  $k_{\text{cat}}$  and  $K_{\text{m}}$  values were determined using 20 mM 2-(*N*-morpholino)ethanesulfonic acid (MES), 50 mM NaCl and 0.1% bovine serum albumin (BSA) at pH 6 and 40 °C. BadX at  $1.5 \times 10^{-4}$  mM was used in the assay and the ONPX<sub>2</sub> concentration varied from 0.1 to  $12 \times K_{\text{m}}$ . The pH-dependence studies were performed at 25 °C with 50 mM NaCl, 0.1% BSA and 20 mM succinic acid (pH 3.0–4.5), 20 mM MES (pH 5.0–6.5), 20 mM (*N*-[2-hydroxyethyl]piperazine-*N'*-[2-ethanesulfonic acid]) (HEPES) (pH 7.0–8.0) or 20 mM 2-(*N*-cyclohexylamino)ethanesulfonic acid (CHES) (pH 8.5–9.0) using  $9.3 \times 10^{-2}$  mM of ONPX<sub>2</sub> with a final BadX concentration of  $3.0 \times 10^{-3}$  mM such that  $\geq 80\%$  of the substrate was depleted. The experimental data were fitted to a pseudo-first-order expression, which upon division by the enzyme concentration yielded  $k_{\text{cat}}/K_{\text{m}}$  values. These  $k_{\text{cat}}/K_{\text{m}}$  values were then fitted against a bell-shaped activity profile. An error in the derived  $\text{p}K_{\text{a}}$  values of  $\pm 0.1$  units is estimated from the error in pH measurements.

#### 4.4. Circular dichroism spectroscopy

Circular dichroism (CD) spectra were measured on a JASCO J-810 spectropolarimeter equipped with a JASCO PFD-425S Peltier heater and a circulating water bath. A 2 mm pathlength cell containing protein at a concentration of  $\sim 0.25$  mg/mL in 10 mM sodium phosphate with and without NaCl was used. Thermal unfolding was monitored at 219 nm using a heating rate of 1 °C/min.

#### 4.5. Irreversible inactivation

BadX and BcX were incubated at 55 °C and pH 6, 8 or 10 in 10 mM sodium phosphate from 0 to 360 s, and aliquots of enzyme were removed at designated time intervals and quenched in ice-cold Eppendorf tubes. When warmed back to room temperature, 20  $\mu\text{L}$  of BadX (final concentration of  $3.2 \times 10^{-3}$  mM) and 10  $\mu\text{L}$  of BcX (final concentration of  $2.9 \times 10^{-3}$  mM) were assayed with 0.093 mM ONPX<sub>2</sub> in 20 mM MES, 50 mM NaCl and 0.1% BSA at pH 6.0 and 20 °C to ascertain residual  $k_{\text{cat}}/K_{\text{m}}$  as a function of incubation time. Data were normalized versus the activity measured before incubation.

#### Acknowledgements

This work was funded by the Government of Canada's Network of Centres of Excellence Program supported by the Canadian Institutes of Health Research (CIHR) and the Natural Sciences and Engineer-

ing Research Council (NSERC) through the Protein Engineering Network of Centres of Excellence (PENCE Inc.). LPM is a CIHR Scientist.

#### References

1. Subramanayan, S.; Prema, P. *FEMS Microbiol. Lett.* **2000**, *183*, 1–7.
2. Kulkarni, N.; Shendye, A.; Rao, M. *FEMS Microbiol. Rev.* **1999**, *23*, 411–456.
3. Törrönen, A.; Rouvinen, J. *J. Biotechnol.* **1997**, *157*, 137–149.
4. Sapag, A.; Wouters, J.; Lambert, C.; de Ioannes, P.; Eyzaguirre, J.; Depiereux, E. *J. Biotechnol.* **2002**, *95*, 109–131.
5. Henrissat, B.; Bairoch, A. *Biochem. J.* **1996**, *316*, 695–696.
6. Henrissat, B. *Biochem. J.* **1991**, *280*, 309–316.
7. Davies, G.; Henrissat, B. *Structure* **1995**, *3*, 853–859.
8. McIntosh, L. P.; Hand, G.; Johnson, P. E.; Joshi, M. D.; Körner, M.; Plesniak, L. A.; Ziser, L.; Wakarchuk, W. W.; Withers, S. G. *Biochemistry* **1996**, *35*, 9958–9966.
9. Joshi, M. D.; Sidhu, G.; Nielsen, J. E.; Brayer, G. D.; Withers, S. G.; McIntosh, L. P. *Biochemistry* **2001**, *40*, 10115–10139.
10. Joshi, M. D.; Sidhu, G.; Pot, I.; Brayer, G. D.; Withers, S. G.; McIntosh, L. P. *J. Mol. Biol.* **2000**, *299*, 255–279.
11. Törrönen, A.; Rouvinen, J. *Biochemistry* **1995**, *34*, 847–856.
12. Kregel, U.; Dijkstra, B. W. *J. Mol. Biol.* **1996**, *263*, 70–78.
13. Fushinobu, S.; Ito, K.; Konno, M.; Wakagi, T.; Matsuzawa, H. *Protein Eng.* **1998**, *11*, 1121–1128.
14. Martins, R. F.; Davids, W.; Al-Soud, W. A.; Levander, F.; Rådström, P.; Hatti-Kaul, R. *Extremophiles* **2001**, *5*, 135–144.
15. Novozymes A/S Product Sheet, Pulpzyme HC, **2002**.
16. Sabini, E.; Sulzenbacher, G.; Dauter, M.; Dauter, Z.; Jørtensen, P. L.; Schülein, M.; Dupont, C.; Davies, G. J.; Wilson, K. S. *Chem. Biol.* **1999**, *6*, 483–492.
17. Sabini, E.; Wilson, K. S.; Danielsen, S.; Schülein, M.; Davies, G. J. *Acta Crystallgr., Sect. D* **2001**, *57*, 1344–1347.
18. Wakarchuk, W. W.; Campbell, R. L.; Sung, W. L.; Davoodi, J.; Yaguchi, M. *Protein Sci.* **1994**, *3*, 467–475.
19. Sidhu, G.; Withers, S. G.; Nguyen, N. T.; McIntosh, L. P.; Ziser, L.; Brayer, G. D. *Biochemistry* **1999**, *38*, 5346–5354.
20. Lawson, S. L.; Wakarchuk, W. W.; Withers, S. G. *Biochemistry* **1996**, *35*, 10110–10118.
21. Davoodi, J.; Wakarchuk, W. W.; Campbell, R. L.; Carey, P. R.; Surewicz, W. K. *Eur. J. Biochem.* **1995**, *232*, 839–843.
22. Nath, D.; Rao, M. *Eur. J. Biochem.* **2001**, *268*, 5471–5478.
23. Nakamura, S.; Aono, R.; Wakabayashi, K.; Horikoshi, K. In *Xylans and Xylanases*; Visser, J.; Beldman, G.; Kusters-Van Someren, M. A.; Voragen, A. G. J., Eds.; Elsevier: Amsterdam, 1992; pp 443–446.
24. Thompson, J. D.; Higgins, D. G.; Gibson, T. J. *Nucleic Acids Res.* **1994**, *22*, 4673–4680.
25. Laskowski, R. A.; MacArthur, M. W.; Moss, D. S.; Thornton, J. M. *J. Appl. Cryst.* **1993**, *26*, 283–291.
26. Shibuya, H.; Kaneko, S.; Hayashi, K. *Biochem. J.* **2000**, *349*, 651–656.

27. Sung, W.L.; Yaguchi, M.; Ishikawa, K. US Patent 5759840.
28. Georis, J.; De Lemos Esteves, F.; Lamotte-Brasseur, J.; Bougnet, V.; Devreese, B.; Giannotta, F.; Granier, B.; Frère, J. M. *Protein Sci.* **2000**, *9*, 466–475.
29. Gruber, K.; Klintschar, G.; Hayn, M.; Schlacher, A.; Steiner, W.; Kratky, C. *Biochemistry* **1998**, *37*, 13475–13485.
30. Plesniak, L. A.; Wakarchuk, W. W.; McIntosh, L. P. *Protein Sci.* **1996**, *5*, 1118–1135.
31. Plesniak, L. A.; Connelly, G. P.; Wakarchuk, W. W.; McIntosh, L. P. *Protein Sci.* **1996**, *5*, 2319–2328.
32. Joshi, M. D.; Hedberg, A.; McIntosh, L. P. *Protein Sci.* **1997**, *6*, 2667–2670.
33. Chakravarty, S.; Varadarajan, R. *Biochemistry* **2002**, *41*, 8152–8161.
34. Ziser, L.; Withers, S. G. *Carbohydr. Res.* **1994**, *265*, 9–17.
35. Ziser, L.; Setyawati, I.; Withers, S. G. *Carbohydr. Res.* **1995**, *274*, 137–153.
36. Pace, C. N.; Vajdos, F.; Fee, L.; Grimsley, G.; Gray, T. *Protein Sci.* **1995**, *4*, 2411–2423.
37. Sung, W. L.; Luk, C. K.; Zahab, D. M.; Wakarchuk, W. *Protein Exp. Purif.* **1993**, *4*, 200–206.
38. Leatherbarrow, R.J. *Gra-Fit, Version 4.0*, **1998**, Erithacus Software Ltd., UK, Staines.